Exploring the photo-toxicity of hypoxic active iridium(III)-based sensitizers in 3D tumor spheroids

Robin Bevernaegie,[†] Bastien Doix,[‡] Estelle Bastien,[‡] Aurélie Diman,[⊥Γ] Anabelle Decottignies, [⊥] Olivier Feron, [‡*] and Benjamin Elias[†*]

† UCLouvain, Institut de la Matière Condensée et des Nanosciences, Molecular Chemistry, Materials and Catalysis, Place Louis Pasteur 1 box L4.01.02, B-1348 Louvain-la-Neuve, Belgium.

‡ UCLouvain, Institut de Recherche Expérimentale et Clinique, Pole of Pharmacology and Therapeutics, Avenue Hippocrate 57 box B1.57.04, B-1200 Woluwé-Saint-Lambert, Belgium.

⊥ UCLouvain, Institut de Duve, Avenue Hippocrate 75 box B1.75.02, B-1200 Woluwé-Saint-Lambert, Belgium.

ABSTRACT: Among all molecules developed for anticancer therapies, photodynamic therapeutic agents have a unique profile. Their maximal activity is specifically triggered in tumors by light and toxicity of even systemically delivered drug is prevented in non-illuminated parts of the body. Photosensitizers exert their therapeutic effect by producing reactive oxygen species via a light-activated reaction with molecular oxygen. Consequently, the lowering of pO_2 deep in solid tumors limits their treatment and makes essential the design of oxygen-independent sensitizers. In this perspective, we have recently developed Ir(III)-based molecules able to oxidize biomolecules by type I processes under free-oxygen conditions. We examine here their photo-toxicity in relevant biological models. We show that drugs, which are mitochondria-accumulated, induce upon light irradiation a dramatic decrease of the cell viability, even under low oxygen conditions. Finally, assays on 3D tumor spheroids highlight the importance of the light-activation step and the oxygen consumption rate on the drug activity.

Introduction

Over the last decades, photodynamic therapy (PDT) has emerged as a promising method to treat diseases in diverse areas of medicine, especially in oncology.[1, 2] Its features, including low systemic toxicity and minimally invasive procedure, make it an interesting alternative to conventional cancer therapies such as chemotherapy, radiotherapy and surgery.[3] The photodynamic effect arises from a light-activated reaction between a photosensitizer (PS) and molecular oxygen.[1-3] The mechanisms are complex but can be divided in two main pathways, both inducing the production of reactive oxygen species (ROS) (**Fig. 1**).[4] On the one hand, type I processes involve a photo-induced electron transfer with biological substrates, leading after several steps to radical species such as superoxide ($O_2^{\bullet-}$), hydroxyl ($OH^{\bullet}$) and hydroperoxyl ($HO_2^{\bullet}$). On the other hand, type II photoreactivity consists in the production of singlet oxygen ($^1O_2$) by a direct energy transfer.

For decades, research in cancer PDT has focused on the design of efficient photosensitizers to produce more $^1O_2$, which is the main mediator causing tissue damage.[4, 5] Different generations of light-activatable molecules with an increased quantum yield of $^1O_2$ photo-production (Φ_Δ) have been developed.[6, 7] Efforts have been also made to improve light-absorption of these compounds in the therapeutic window (600-1000 nm) and thereby to reach deep-seated solid tumors. Unfortunately, the lowering of tumor pO_2 at distance from blood vessels remains an obstacle for the use of classical photosensitizers because of the need of PDT for molecular oxygen to initiate cell death.[8-10] Recent studies have however shown that type I photoreactivity can lead to strong cytotoxic effects under low oxygen conditions.[11-18] Innovative strategies, involving this pathway, have thus recently been developed to overcome the problem of tumor hypoxia.[8] Nevertheless, it remains an under-explored research area and hypoxic active type I photosensitizers are still scarcely-reported.

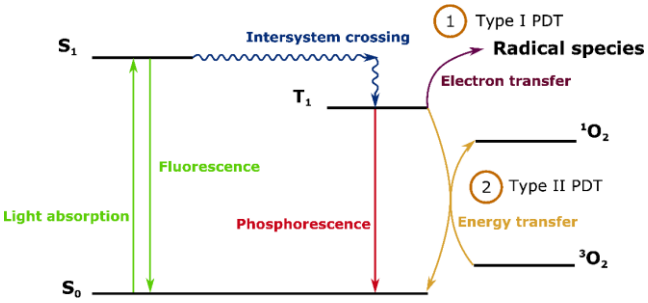

Figure 1. Simplified Jablonski diagram for classical production of ROS by a photosensitizer through type I (purple) and type II photoprocesses (yellow).

Consequently, we have concentrated our efforts on developing novel molecules able to cause cellular damage by exploiting type I processes. We have opted for bis-cyclometalated Ir(III) complexes because they form lipophilic cations characterized by a rapid cellular uptake[19-21] and tunable redox properties.[22-24] Actually, we have recently reported on novel Ir(III)-based compounds with long-lived triplet excited states[25] and strong photo-oxidizing powers.[26] Our goal is now to examine whether the intracellular oxygen content influences their photo-cytotoxicity. Viability assays have been performed on 2D cell cultures under both normoxic and hypoxic conditions as well as on 3D tumor spheroids. These models are particularly

suited for this study, due to the development of a spontaneous hypoxic core.[27]

Results and discussion

Two Ir(III) complexes, namely **Ir-pzpy** and **Ir-TAP** (**Fig. 2**), have been synthetized and purified as previously described (Supporting information).[25, 26] Confocal microscopy of FaDu cancer cells (**Fig. 2**) reveals a rapid uptake of both compounds upon 1h incubation time. Co-localization experiments with subcellular markers show that these drugs are mainly mitochondria-accumulated (Pearson's correlation coefficient of 0.81 and 0.93 for **Ir-pzpy** and **Ir-TAP** respectively), which is consistent with many other examples of positively-charged Ir(III) complexes, reaching these organelles by energy-dependent or independent pathways.[28-31] Such a subcellular localization may actually constitute a key feature for Ir(III)-based molecules through the induction of mitochondrial dysfunction and associated cell death pathways, as reported for various mitochondria-targeting compounds.[32, 33]

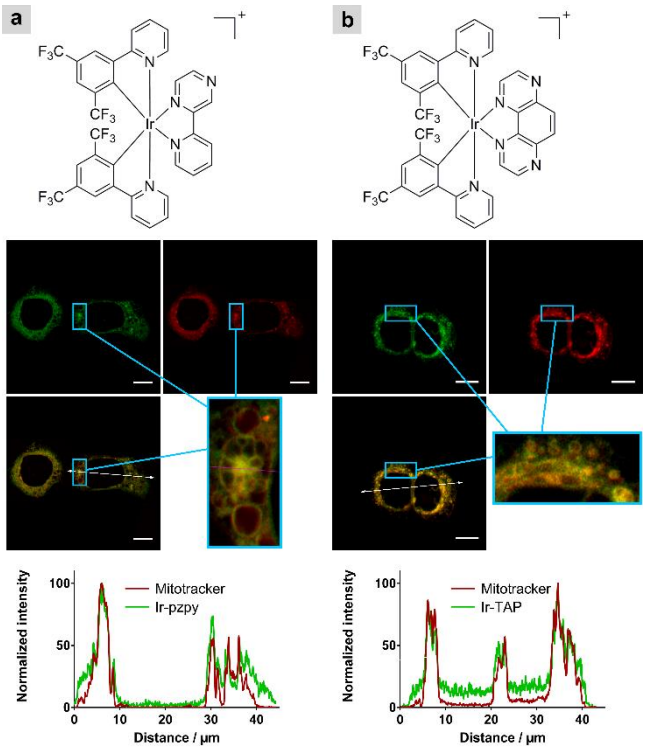

Figure 2. Live confocal imaging of FaDu cancer cells after 1h incubation with 20 µM of (a) **Ir-pzpy** and (b) **Ir-TAP**. The Ir(III) photosensitizers are in green and the Mitotracker Red CMXROS is in red. A plot profile across the cell (white arrow) is also shown for each photosensitizer. Scale bars: 100 µM.

The capacity of both Ir(III)-based drugs to initiate cell death has been assessed on FaDu and HT-29 cancer cells, under normoxic (21% O_2) and hypoxic (1% O_2) conditions. The IC_{50} values (**Table 1**), obtained by plotting viability *vs.* log concentration (**Fig. S1**), show that whereas the dark toxicity of both complexes is relatively low in the studied concentration range, cell viability decreases dramatically upon light excitation (light dose = 2.83 J/cm^2). This light-triggered cytotoxic effect though reduced at lower pO_2 due to the inhibition of type II photoprocesses, is still significant for both compounds under hypoxia, which supports possible contribution of oxygen-independent type I processes. Interestingly, lowering pO_2 affects in a different way the photo-cytotoxicity of both sensitizers, with hypoxia/normoxia IC_{50} ratio amounting to 3.3-4.8 for **Ir-pzpy** and 2.0-2.4 for **Ir-TAP** upon light excitation. A possible explanation for this phenomenon arises from the longer excited state lifetime of **Ir-pzpy** in water ($\tau_{\text{Ir-pzpy}}$ = 297 ns) as compared to **Ir-TAP** ($\tau_{\text{Ir-TAP}}$ = 56 ns) and thus its stronger sensitivity towards the amount of dissolved oxygen. This result reflects the better capacity of **Ir-pzpy** to generate $^1O_2$ through a type II photoreaction and is consistent with the $^1O_2$ quantum yields, determined for each complex in water (Φ_Δ **Ir-pzpy** = 0.68, Φ_Δ **Ir-TAP** = 0.08) (**Fig. S2** and **Table S1**). These data support a model wherein the anticancer activity of **Ir-pzpy** relies more on a classical type II PDT pathway than the one of **Ir-TAP**, which exhibits thus a stronger cytotoxic activity in the absence of oxygen.

Table 1. IC_{50} values[a] determined from dose-dependent growth inhibitory curves of Ir-pzpy and Ir-TAP on FaDu and HT-29 cancer cells, in the dark and upon light activation, under normoxic (21% O_2) and hypoxic (1% O_2) conditions. Cells were treated during 1h with the desired concentration of complex, before being irradiated or not for 30 min with 405nm-LEDs (light dose = 2.83 J/cm^2). The amount of viable cells was determined 24h later by WST-1 viability assays.

Cell type		**Ir-pzpy** / µM		**Ir-TAP** / µM	
		Light (Dark)	PI[b]	Light (Dark)	PI[b]
FaDu	Normoxia	3.8±0.4 (69.4±6.2)	18.4	5.4±0.4 (> 100)	> 18.5
	Hypoxia	18.1±1.8 (79.6±7.1)	4.4	12.8±0.7 (> 100)	> 7.8
HT-29	Normoxia	8.7±0.7 (> 100)	> 11.5	12.0±0.5 (> 100)	> 8.3
	Hypoxia	28.6±2.3 (96.2±6.2)	3.4	24.2±1.5 (> 100)	> 4.3

[a] The data obtained in three independent experiments (4 wells/condition) are expressed as mean + standard deviation. [b] PI = photoindex = IC_{50} dark/IC_{50} light

The above hypothesis has been confirmed by photocleavage experiments carried out on a supercoiled pBR322 plasmid (**Fig. 3**). While both drugs are inactive in the dark, **Ir-pzpy** shows a strong cleavage activity upon 30 min irradiation with 405nm-LEDs (**Fig. 3**). Indeed, at concentrations exceeding 10 µM, the bands attributed to the supercoiled conformation disappear whereas open-circular as well as linear plasmid conformations appear (lane 5-10) (**Fig. 3a**). However, as expected from the model described above, the addition of a singlet oxygen scavenger (NaN_3) decreases dramatically the cleavage activity of **Ir-pzpy**. Only the open-circular conformation is obtained and it coexists with the supercoiled form, even at the highest complex concentrations. By contrast, the photocleavage activity of **Ir-TAP** though reduced due to its shorter excited state lifetime, is less affected by the addition of sodium azide. With or without the singlet oxygen scavenger, the supercoiled conformation is always present and only the open-circular form can be obtained (**Fig. 3b**). This result is consistent with its lower $^1O_2$ quantum yield as compared to **Ir-**

pzpy. Finally, it is worth noting that these experiments demonstrate unambiguously that the PDT activity of both complexes does not only rely on $^1O_2$ sensitization but also involves type I processes.

In order to explore the cell death mechanism initiated by Ir(III) complexes upon light excitation, flow cytometric analyses of FaDu cancer cells double-labeled with Annexin V-FITC and propidium iodide have been performed (**Fig. S3-S4**). As shown in the supporting information, no-treated cells remain viable, with cell mortality inferior to 10%. By contrast, treatments with **Ir-pzpy** and **Ir-TAP** induce cytotoxicity, which increases with the drug dose as well as over the time after the irradiation step. For both drugs, at intermediate concentrations, early apoptosis is detected, which suggests that cell mortality mainly occurs by apoptotic pathways.

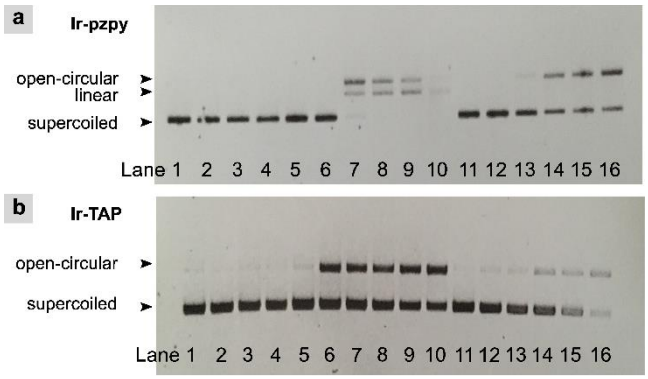

Figure 3. Agarose (0.8%) gel electrophoresis of supercoiled pBR322 plasmid DNA (260 ng) exposed to (a) **Ir-pzpy** for 30 min and (b) **Ir-TAP** for 120 min. Lane 1: pBR322 control dark, Lane 2: pBR322 control + NaN_3 (10 mM) dark, Lane 3: pBR322 + **Ir** (25 µM) dark, Lane 4: pBR322 + **Ir** (25 µM) + NaN_3 (10 mM) dark, Lane 5-10: pBR322 + **Ir** (0, 5, 10, 15, 20, 25 µM) light, Lane 11-16: pBR322 + **Ir** (0, 5, 10, 15, 20, 25 µM) + NaN_3 (10 mM) light.

In addition to the experiments conducted on 2D cancer cell monolayers, the oxygen-dependence of the Ir(III) complexes anticancer activity has also been examined in 3D tumor spheroids. As proven in the supporting information (**Fig. S5**), FaDu tumor spheroids are characterized by the development of a spontaneous hypoxic core surrounded by a normoxic continuum, thereby recapitulating the different compartments, with lower or higher oxygen levels, observed in a tumor *in vivo*. Moreover, matrix and cell-cell interactions within these 3D multicellular aggregates make them particularly suited to study drug penetration and, in the specific context of photosensitizers, to evaluate the capacity of light to reach them deep in the tissues.[27, 34]

Viability assays performed on 3D tumor spheroids confirm the primary conclusions drawn from the experiments conducted on 2D cell cultures. Whereas the cytotoxicity of both drugs is weak in the dark (**Fig. 4a** and **Fig. S7**), the light activation (light dose = 2.83 J/cm^2) induces a dramatic decrease in cancer cell viability (**Fig. 4b** and **Fig. S8**). Importantly, the effects of both complexes are consistent with results obtained with cell monolayers under hypoxia. Indeed, **Ir-TAP** shows larger growth inhibitory effects towards tumor spheroids than **Ir-pzpy**, which supports a pronounced activity of the former when hypoxia is present in the system. The cell death associated to the photo-toxicity of **Ir-pzpy** is actually limited to surface cell layers and does not vary a lot with the drug concentration (**Fig. 4b-4c** and **Fig. S7**). By contrast, the cytotoxic effects, arising from light-activated **Ir-TAP**, are detected deep in the 3D cellular aggregates, even in strong hypoxic areas (**Fig. 4b-4c** and **Fig. S8**).

A lack of light penetration cannot account for the failure of **Ir-pzpy** to inhibit the spheroid growth. Indeed, although both complexes possess the same absorption properties on the excitation wavelength ($\varepsilon_{405\ nm}$ = ± 800 $M^{-1}.cm^{-1}$ for both compounds) (**Fig. S11**), **Ir-TAP** (20 µM) can induce the complete destruction of the spheroidal structure and has therefore a stronger photo-activity than **Ir-pzpy** at the same concentration. In addition, a problem of drug penetration can be excluded because luminescent signals arising from each Ir(III) complex have been observed at different depths in the 3D multicellular aggregates. These luminescent signals are actually homogeneously distributed in the different z-stacks analyzed by confocal microscopy (**Fig. S12**), but also over whole deep-seated sections obtained by physical slicing of FaDu tumor spheroids (**Fig. 4d-4e**).

The incomplete destruction of spheroids by **Ir-pzpy** is likely to be associated to its stronger sensitivity to oxygen and its subsequent higher dependence on type II processes. In 3D multicellular models, such a phenomenon has already been reported on several well-known PDT sensitizers, including Photofrin, 5-aminolevulinic acid (ALA) and hypericin.[35-38] Actually, whereas the supply of oxygen is limited in tumor spheroids, the photo-production of $^1O_2$ by these compounds induces a rapid depletion of pO_2 inside the 3D structure. Consequently, the anticancer activity of strong type II sensitizers, such as those mentioned above and **Ir-pzpy**, decreases dramatically. Usually, a reduction of the light dose leads to the recovery of their antiproliferative effect by diminishing the oxygen consumption rate. Fractional photodynamic therapy may also be considered for these compounds.[39] However, as reported by Evans *et al.*,[40] the use of type I sensitizers represents another promising approach. Indeed, thanks to their lower oxygen consumption rate and their ability to induce cellular damage at low pO_2, they show a great activity in 3D tumor spheroids. Such a behavior is verified herein with **Ir-TAP**, which is characterized by a high photo-oxidizing power as well as a low $^1O_2$ quantum yield and which presents an exquisite therapeutic effect in spontaneously hypoxic spheroids models.

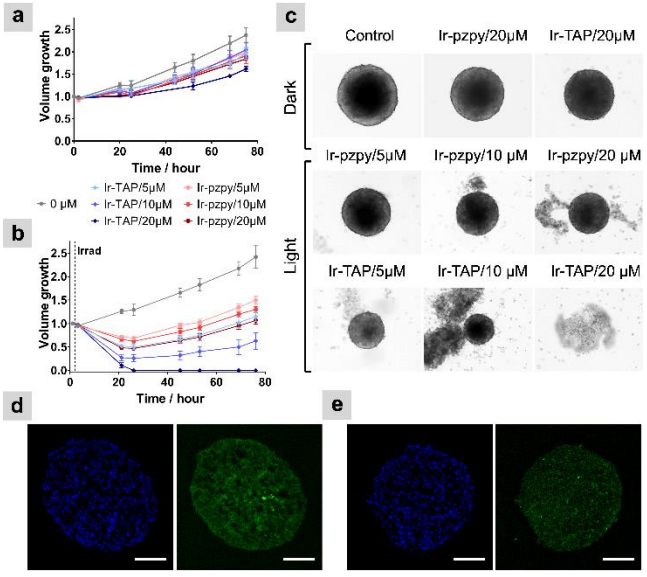

Figure 4. (a) Dark and (b) light-induced cytotoxic effect of **Ir-pzpy** and **Ir-TAP** on tumor spheroids (diameter: 350-400 µm) obtained from 3D cultures of FaDu cancer cells. A timeline summarizing this experiment is given in **Fig. S6**. The volume growth of spheroids is plotted as a function of time. At day 5, the spheroids were incubated without drugs or with **Ir-pzpy** or **Ir-TAP** for 24h. They were then exposed (t = 1h) or not to 405nm-LEDs for 30 min (light dose = 2.83 J/cm^2). (c) Representative pictures of 3D FaDu tumor spheroids 24h after the irradiation step. (d-e) Representative picture of sections (5 µm), obtained by physical slicing of FaDu tumor spheroids after 24h incubation with 20 µM of (d) **Ir-pzpy** and (e) **Ir-TAP**. The Ir(III)-based photosensitizers are in green and nuclei were stained with Draq5 in blue. Scale bars: 100 µm.

In order to increase the growth inhibitory effect of **Ir-pzpy**, fractional PDT with two irradiation steps (light dose/irradiation = 2.83 J/cm^2) at 24h interval has been carried out. As expected, an additional reduction in the spheroid volume has been observed due to tissue reoxygeneation (**Fig. 5a-5b** and **Fig. S10**). In addition, it is worth noting that the combination of two separated irradiation steps at a lower drug concentration (10 µM) has been found to be more efficient than a single irradiation step at a higher concentration (20 µM). A similar experiment has also been performed using **Ir-TAP** as photosensitizer. In this case, fractional PDT has allowed us to decrease the drug concentration used from 20 µM to 10 µM, whilst keeping an important cytotoxic effect and inducing the complete destruction of the 3D multicellular aggregates (**Fig. 5a-6b** and **Fig. S10**).

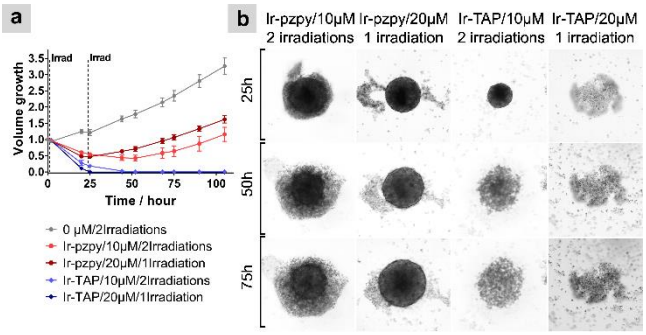

Figure 5. (a) Cytotoxic effect of **Ir-pzpy** and **Ir-TAP** on tumor spheroids (diameter: 350-400 µm) obtained from 3D cultures of FaDu cancer cells. A timeline summarizing this experiment is given in **Fig. S9**. The volume growth of spheroids is plotted as a function of time. At day 5, spheroids were incubated without drugs or with **Ir-pzpy** or **Ir-TAP** for 24h. They were then exposed once (t = 1h) (light dose = 2.83 J/cm^2) or twice (t = 1h and 24h) (light dose = 5.66 J/cm^2) to 405nm-LEDs for 30 min. (b) Representative pictures of 3D FaDu tumor spheroids at different time.

Conclusion

In conclusion, we showed that photo-oxidizing iridium(III) complexes represent an attractive family of photosensitizers to treat tumors. Indeed, as reported for other Ir(III)-based compounds, they are characterized by a rapid cellular uptake and the capacity to penetrate deep into 3D tumor spheroids.[41-43] In addition, thanks to their subcellular localization, they are able to induce rapid apoptotic cell death upon light excitation. Between the two Ir(III)-based drugs studied here, **Ir-TAP** has emerged as the most promising candidate by combining a low $^1O_2$ quantum yield and the capacity to initiate type I oxygen-independent processes. A complete destruction of 3D tumor spheroids has been observed at a concentration of 20 µM, but also at 10 µM in combination with two irradiation steps at 24h interval. By contrast, the therapeutic activity of the second compound, **Ir-pzpy**, remains limited in such models. Actually, this phenomenon has been attributed to its rapid consumption of all the oxygen available in the spheroid, as previously proven for other strong $^1O_2$ sensitizers. However, thanks to fractional PDT, an increased growth inhibitory effect could be obtained with **Ir-pzpy**.

These results open the door to future studies investigating the anticancer effect of both drugs *in vivo*. Nevertheless, in this context, the short activation wavelength (405 nm) of our drugs might be an issue when it comes to light penetration in living tissues. Consequently, the use of two-photon excitation will also be examined. Indeed, several recent studies have shown that photo-cytotoxic Ir(III) complexes could be excited through the absorption of two low-energy photons instead of one high-energy photon.[44-50]

ASSOCIATED CONTENT

Experimental and synthetic details, 2D cell viability curves, Representative pictures of 3D tumor spheroids, $^1O_2$ quantum yields data, UV-visible spectra of **Ir-pzpy** and **Ir-TAP** and additional confocal imaging.
The Supporting Information is available free of charge on the ACS Publications website.

AUTHOR INFORMATION

Corresponding Author

* Prof. Benjamin Elias, UCLouvain, Institut de la Matière Condensée et des Nanosciences (IMCN), Place Louis Pasteur 1 box L4.01.02, B-1348 Louvain-la-Neuve, Belgium, E-mail: benjamin.elias@uclouvain.be
* Prof. Olivier Feron, UCLouvain, Institut de Recherche Expérimentale et Clinique (IREC), Avenue Hippocrate 57 box B1.57.04, B-1200 Woluwé-Saint-Lambert, Belgium, E-mail: olivier.feron@uclouvain.be

Present Addresses

Γ Department of Microbiology and Molecular Medicine, University Medical Centre (C.M.U.), Rue Michel-Servet 1, 1211 Geneva 4, Switzerland.

Author Contributions

All authors have given approval to the final version of the manuscript.

Notes

The authors declare no competing financial interests.

ACKNOWLEDGMENT

This work was supported by the Fonds National pour la Recherche Scientifique (F.R.S.-FNRS) (Grant n°J.0091.18). R.B. and B.E. gratefully acknowledge the Fonds pour la Formation à la Recherche dans l'Industrie et dans l'Agriculture (F.R.I.A.), the Région Wallonne, the UCLouvain and the Prix Pierre et Colette Bauchau for financial support. In the O.F. lab, this work was supported by grants from the Belgian Foundation against cancer (#2016-101, #2016-085) and an Action de Recherche Concertée (ARC 14/19-058). Prof. F. Loiseau is thanked for her help with the measurement of luminescence lifetimes. M.-C. Eloy is deeply thanked for her help with the confocal microscopy experiments.

REFERENCES

1. Brian, C. W.; Michael, S. P. The physics, biophysics and technology of photodynamic therapy. *Physics in Medicine & Biology* **2008,** 53, R61.
2. Agostinis, P.; Berg, K.; Cengel, K. A.; Foster, T. H.; Girotti, A. W.; Gollnick, S. O.; Hahn, S. M.; Hamblin, M. R.; Juzeniene, A.; Kessel, D.; Korbelik, M.; Moan, J.; Mroz, P.; Nowis, D.; Piette, J.; Wilson, B. C.; Golab, J. Photodynamic therapy of cancer: An update. *CA: A Cancer Journal for Clinicians* **2011,** 61, 250-281.
3. Bown, S. G. Photodynamic therapy for photochemists. *Philos. Trans. R. Soc., A* **2013,** 371.
4. Mroz, P.; Yaroslavsky, A.; Kharkwal, G. B.; Hamblin, M. R. Cell Death Pathways in Photodynamic Therapy of Cancer. *Cancers* **2011,** 3, 2516.
5. Castano, A. P.; Mroz, P.; Hamblin, M. R. Photodynamic therapy and anti-tumour immunity. *Nature Reviews Cancer* **2006,** 6, 535.
6. Ormond, A.; Freeman, H. Dye Sensitizers for Photodynamic Therapy. *Materials* **2013,** 6, 817.
7. Monro, S.; Colon, K. L.; Yin, H.; Roque, J., 3rd; Konda, P.; Gujar, S.; Thummel, R. P.; Lilge, L.; Cameron, C. G.; McFarland, S. A. Transition Metal Complexes and Photodynamic Therapy from a Tumor-Centered Approach: Challenges, Opportunities, and Highlights from the Development of TLD1433. *Chem. Rev.* **2019,** 119, 797-828.
8. Li, X.; Kwon, N.; Guo, T.; Liu, Z.; Yoon, J. Innovative Strategies for Hypoxic-Tumor Photodynamic Therapy. *Angew. Chem. Int. Ed. Engl.* **2018,** 57, 11522-11531.
9. Wilson, W. R.; Hay, M. P. Targeting hypoxia in cancer therapy. *Nature Reviews Cancer* **2011,** 11, 393.
10. Pinto, A.; Mace, Y.; Drouet, F.; Bony, E.; Boidot, R.; Draoui, N.; Lobysheva, I.; Corbet, C.; Polet, F.; Martherus, R.; Deraedt, Q.; Rodríguez, J.; Lamy, C.; Schicke, O.; Delvaux, D.; Louis, C.; Kiss, R.; Kriegsheim, A. V.; Dessy, C.; Elias, B.; Quetin-Leclercq, J.; Riant, O.; Feron, O. A new ER-specific photosensitizer unravels 1O2-driven protein oxidation and inhibition of deubiquitinases as a generic mechanism for cancer PDT. *Oncogene* **2015,** 35, 3976.
11. Lv, Z.; Wei, H.; Li, Q.; Su, X.; Liu, S.; Zhang, K. Y.; Lv, W.; Zhao, Q.; Li, X.; Huang, W. Achieving efficient photodynamic therapy under both normoxia and hypoxia using cyclometalated Ru(ii) photosensitizer through type I photochemical process. *Chem. Sci.* **2018,** 9, 502-512.
12. Ding, H.; Yu, H.; Dong, Y.; Tian, R.; Huang, G.; Boothman, D. A.; Sumer, B. D.; Gao, J. Photoactivation switch from type II to type I reactions by electron-rich micelles for improved photodynamic therapy of cancer cells under hypoxia. *J. Controlled Release* **2011,** 156, 276-280.
13. Gilson, R. C.; Black, K. C. L.; Lane, D. D.; Achilefu, S. Hybrid TiO2–Ruthenium Nano-photosensitizer Synergistically Produces Reactive Oxygen Species in both Hypoxic and Normoxic Conditions. *Angew. Chem. Int. Ed.* **2017,** 56, 10717-10720.
14. Arenas, Y.; Monro, S.; Shi, G.; Mandel, A.; McFarland, S.; Lilge, L. Photodynamic inactivation of Staphylococcus aureus and methicillin-resistant Staphylococcus aureus with Ru(II)-based type I/type II photosensitizers. *Photodiagnosis and Photodynamic Therapy* **2013,** 10, 615-625.
15. Lameijer, L. N.; Ernst, D.; Hopkins, S. L.; Meijer, M. S.; Askes, S. H. C.; Le Dévédec, S. E.; Bonnet, S. A Red-Light-Activated Ruthenium-Caged NAMPT Inhibitor Remains Phototoxic in Hypoxic Cancer Cells. *Angew. Chem. Int. Ed.* **2017,** 56, 11549-11553.
16. Novohradsky, V.; Rovira, A.; Hally, C.; Galindo, A.; Vigueras, G.; Gandioso, A.; Svitelova, M.; Bresolí-Obach, R.; Kostrhunova, H.; Markova, L.; Kasparkova, J.; Nonell, S.; Ruiz, J.; Brabec, V.; Marchán, V. Towards Novel Photodynamic Anticancer Agents Generating Superoxide Anion Radicals: A Cyclometalated IrIII Complex Conjugated to a Far-Red Emitting Coumarin. *Angew. Chem. Int. Ed.* **2019,** 58, 6311-6315.
17. Novohradsky, V.; Vigueras, G.; Pracharova, J.; Cutillas, N.; Janiak, C.; Kostrhunova, H.; Brabec, V.; Ruiz, J.; Kasparkova, J. Molecular superoxide radical photogeneration in cancer cells by dipyridophenazine iridium(iii) complexes. *Inorg. Chem. Front.* **2019,** 6, 2500-2513.
18. He, L.; Zhang, M.-F.; Pan, Z.-Y.; Wang, K.-N.; Zhao, Z.-J.; Li, Y.; Mao, Z.-W. A mitochondria-targeted iridium(iii)-based photoacid generator induces dual-mode photodynamic damage within cancer cells. *Chem. Commun.* **2019,** 55, 10472-10475.
19. Caporale, C.; Massi, M. Cyclometalated iridium(III) complexes for life science. *Coord. Chem. Rev.* **2018,** 363, 71-91.
20. McKenzie, L. K.; Bryant, H. E.; Weinstein, J. A. Transition metal complexes as photosensitisers in one- and two-photon photodynamic therapy. *Coord. Chem. Rev.* **2019,** 379, 2-29.
21. Zamora, A.; Vigueras, G.; Rodríguez, V.; Santana, M. D.; Ruiz, J. Cyclometalated iridium(III) luminescent complexes in therapy and phototherapy. *Coord. Chem. Rev.* **2018,** 360, 34-76.
22. Deaton, J. C.; Castellano, F. N. In *Iridium(III) in Optoelectronic and Photonics Applications*; Zysman-Colman, E., Ed.; 2017 John Wiley & Sons Ltd.: 2017; pp 1-69.
23. Weynand, J.; Bonnet, H.; Loiseau, F.; Ravanat, J. L.; Dejeu, J.; Defrancq, E.; Elias, B. Targeting G-Rich DNA Structures with Photoreactive Bis-Cyclometallated Iridium(III) Complexes. *Chemistry* **2019,** 25, 12730-12739.
24. Lentz, C.; Schott, O.; Auvray, T.; Hanan, G.; Elias, B. Photocatalytic Hydrogen Production Using a Red-Absorbing Ir(III)-Co(III) Dyad. *Inorg. Chem.* **2017,** 56, 10875-10881.
25. Bevernaegie, R.; Marcelis, L.; Moreno-Betancourt, A.; Laramee-Milette, B.; Hanan, G. S.; Loiseau, F.; Sliwa, M.; Elias, B. Ultrafast charge transfer excited state dynamics in trifluoromethyl-substituted iridium(iii) complexes. *Phys. Chem. Chem. Phys.* **2018,** 20, 27256-27260.
26. Bevernaegie, R.; Marcélis, L.; Laramée-Milette, B.; De Winter, J.; Robeyns, K.; Gerbaux, P.; Hanan, G. S.; Elias, B. Trifluoromethyl-Substituted Iridium(III) Complexes: From Photophysics to Photooxidation of a Biological Target. *Inorg. Chem.* **2018,** 57, 1356-1367.
27. Kimlin, L. C.; Casagrande, G.; Virador, V. M. In vitro three-dimensional (3D) models in cancer research: An update. *Molecular Carcinogenesis* **2013,** 52, 167-182.
28. Wang, B.; Liang, Y.; Dong, H.; Tan, T.; Zhan, B.; Cheng, J.; Lo, K. K.-W.; Lam, Y. W.; Cheng, S. H. A Luminescent Cyclometalated Iridium(III) Complex Accumulates in Mitochondria and Induces Mitochondrial Shortening by Conjugation to Specific Protein Targets. *ChemBioChem* **2012,** 13, 2729-2737.
29. Cao, J. J.; Tan, C. P.; Chen, M. H.; Wu, N.; Yao, D. Y.; Liu, X. G.; Ji, L. N.; Mao, Z. W. Targeting cancer cell metabolism with mitochondria-immobilized phosphorescent cyclometalated iridium(iii) complexes. *Chem Sci* **2017,** 8, 631-640.
30. Ouyang, M.; Zeng, L.; Huang, H.; Jin, C.; Liu, J.; Chen, Y.; Ji, L.; Chao, H. Fluorinated cyclometalated iridium(iii) complexes as mitochondria-targeted theranostic anticancer agents. *Dalton Trans* **2017,** 46, 6734-6744.
31. Lo, K. K.-W.; Chan, B. T.-N.; Liu, H.-W.; Zhang, K. Y.; Li, S. P.-Y.; Tang, T. S.-M. Cyclometalated iridium(iii) polypyridine dibenzocyclooctyne complexes as the first phosphorescent bioorthogonal probes. *Chem. Commun.* **2013,** 49, 4271-4273.
32. Chakrabortty, S.; Agrawalla, B. K.; Stumper, A.; Vegi, N. M.; Fischer, S.; Reichardt, C.; Kögler, M.; Dietzek, B.; Feuring-Buske, M.; Buske, C.; Rau, S.; Weil, T. Mitochondria Targeted Protein-Ruthenium Photosensitizer for Efficient Photodynamic Applications. *J. Am. Chem. Soc.* **2017,** 139, 2512-2519.
33. Battogtokh, G.; Ko, Y. T. Mitochondrial-targeted photosensitizer-loaded folate-albumin nanoparticle for photodynamic therapy of cancer. *Nanomedicine: Nanotechnology, Biology and Medicine* **2017,** 13, 733-743.
34. Doix, B.; Bastien, E.; Rambaud, A.; Pinto, A.; Louis, C.; Grégoire, V.; Riant, O.; Feron, O. Preclinical Evaluation of White Led-Activated Non-porphyrinic Photosensitizer OR141 in 3D Tumor Spheroids and Mouse Skin Lesions. *Frontiers in Oncology* **2018,** 8.
35. Hilf, R.; Gibson, S. L.; Foster, T. H. *Mechanisms contributing to optimization of PDT with first-generation photosensitizers*. SPIE: 1993; Vol. 1881.
36. Madsen, S. J.; Sun, C.-H.; Tromberg, B. J.; Wallace, V. P.; Hirschberg, H. Photodynamic Therapy of Human Glioma Spheroids Using 5-Aminolevulinic Acid. *Photochem. Photobiol.* **2000,** 72, 128-134.
37. Kamuhabwa, A. A.; Huygens, A.; De Witte, P. A. Photodynamic therapy of transitional cell carcinoma multicellular tumor spheroids with hypericin. *Int. J. Oncol.* **2003,** 23, 1445-50.
38. Kamuhabwa, A. R.; Huygens, A.; Roskams, T.; De Witte, P. A. Enhancing the photodynamic effect of hypericin in human bladder transitional cell carcinoma spheroids by the use of the oxygen carrier, perfluorodecalin. *Int. J. Oncol.* **2006,** 28, 775-80.
39. Weston, M. A.; Patterson, M. S. Validation and Application of a Model of Oxygen Consumption and Diffusion During Photodynamic Therapy In Vitro. *Photochem. Photobiol.* **2014,** 90, 1359-1367.

40. Evans, C. L.; Abu-Yousif, A. O.; Park, Y. J.; Klein, O. J.; Celli, J. P.; Rizvi, I.; Zheng, X.; Hasan, T. Killing Hypoxic Cell Populations in a 3D Tumor Model with EtNBS-PDT. *PLOS ONE* **2011,** 6, e23434.
41. Sun, L.; Li, G.; Chen, X.; Chen, Y.; Jin, C.; Ji, L.; Chao, H. Azo-Based Iridium(III) Complexes as Multicolor Phosphorescent Probes to Detect Hypoxia in 3D Multicellular Tumor Spheroids. *Scientific Reports* **2015,** 5, 14837.
42. Sun, L.; Chen, Y.; Kuang, S.; Li, G.; Guan, R.; Liu, J.; Ji, L.; Chao, H. Iridium(III) Anthraquinone Complexes as Two-Photon Phosphorescence Probes for Mitochondria Imaging and Tracking under Hypoxia. *Chem. Eur. J.* **2016,** 22, 8955-8965.
43. Zhang, P.; Huang, H.; Banerjee, S.; Clarkson, G. J.; Ge, C.; Imberti, C.; Sadler, P. J. Nucleus-Targeted Organoiridium-Albumin Conjugate for Photodynamic Cancer Therapy. *Angew. Chem. Int. Ed. Engl.* **2019,** 58, 2350-2354.
44. Zhou, Z.; Liu, J.; Rees, T. W.; Wang, H.; Li, X.; Chao, H.; Stang, P. J. Heterometallic Ru–Pt metallacycle for two-photon photodynamic therapy. *Proceedings of the National Academy of Sciences* **2018,** 115, 5664-5669.
45. Starkey, J. R.; Pascucci, E. M.; Drobizhev, M. A.; Elliott, A.; Rebane, A. K. Vascular targeting to the SST2 receptor improves the therapeutic response to near-IR two-photon activated PDT for deep-tissue cancer treatment. *Biochimica et Biophysica Acta (BBA) - General Subjects* **2013,** 1830, 4594-4603.
46. Starkey, J. R.; Rebane, A. K.; Drobizhev, M. A.; Meng, F.; Gong, A.; Elliott, A.; McInnerney, K.; Spangler, C. W. New Two-Photon Activated Photodynamic Therapy Sensitizers Induce Xenograft Tumor Regressions after Near-IR Laser Treatment through the Body of the Host Mouse. *Clinical Cancer Research* **2008,** 14, 6564-6573.
47. Samkoe, K. S.; Clancy, A. A.; Karotki, A.; Wilson, B. C.; Cramb, D. T. Complete blood vessel occlusion in the chick chorioallantoic membrane using two-photon excitation photodynamic therapy: implications for treatment of wet age-related macular degeneration. *Journal of Biomedical Optics* **2007,** 12, 1-14, 14.
48. McKenzie, L. K.; Sazanovich, I. V.; Baggaley, E.; Bonneau, M.; Guerchais, V.; Williams, J. A. G.; Weinstein, J. A.; Bryant, H. E. Metal Complexes for Two-Photon Photodynamic Therapy: A Cyclometallated Iridium Complex Induces Two-Photon Photosensitization of Cancer Cells under Near-IR Light. *Chem. Eur. J.* **2017,** 23, 234-238.
49. Qiu, K.; Ouyang, M.; Liu, Y.; Huang, H.; Liu, C.; Chen, Y.; Ji, L.; Chao, H. Two-photon photodynamic ablation of tumor cells by mitochondria-targeted iridium(iii) complexes in aggregate states. *Journal of Materials Chemistry B* **2017,** 5, 5488-5498.
50. Liu, J.; Jin, C.; Yuan, B.; Liu, X.; Chen, Y.; Ji, L.; Chao, H. Selectively lighting up two-photon photodynamic activity in mitochondria with AIE-active iridium(iii) complexes. *Chem. Commun.* **2017,** 53, 2052-2055.

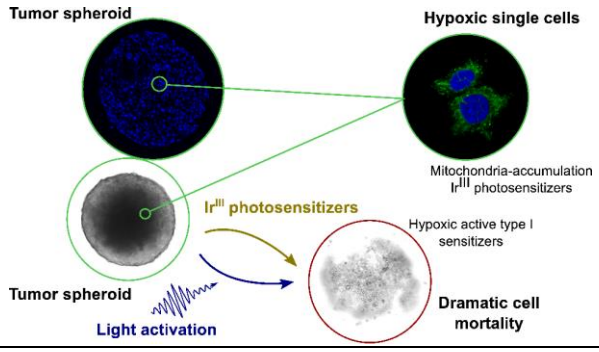
Tumor spheroid
Hypoxic single cells
Mitochondria-accumulation
Ir^{III} photosensitizers
Ir^{III} photosensitizers
Hypoxic active type I
sensitizers
Tumor spheroid
Light activation
Dramatic cell
mortality